Supplementary Information

Understanding coalescence of phase separated droplets and verification via growing a single suspended crystal

Zi-Qing Wu[1†], Yong-Ming Liu[1†], Qing-Di Cheng[1,2†], Chen-Yuan Li[1], Liang-Liang Chen[1], Ya-Li Liu[1], Wan-Yi Ge[1], Sven Falke[2], Hevila Brognaro[2], Jing-Jie Chen[1], Feng-Zhu Zhao[1], Huan Zhou[3], Chen-Yan Zhang[1], Xu-Dong Deng[1], Ya-Jing Ye[1], Wen-Juan Lin[1], Wei-Hong Guo[1], Peng Shang[1,4], Jian-Hua He[3*], Christian Betzel[2*] & Da-Chuan Yin[1,4*]

[1]Key Laboratory for Space Bioscience and Space Biotechnology, School of Life Sciences, Northwestern Polytechnical University, Xi'an 710072, Shaanxi, PR China

[2]Laboratory for Structural Biology of Infection & Inflammation, Institute for Biochemistry and Molecular Biology, University of Hamburg, Hamburg 22607, Germany

[3]Shanghai Institute of Applied Physics, Chinese Academy of Sciences, Shanghai 201204, P.R. China

[4]Shenzhen Research Institute of Northwestern Polytechnical University, Shenzhen 518057, Guangzhou, PR China.

[†] These authors contributed equally to this this work.

*e-mail: yindc@nwpu.edu.cn; betzel@uni-hamburg.de; hejianhua@sinap.ac.cn

This PDF file includes:

Supplementary Derivations 1-2

Supplementary Tables 1-5

Supplementary Movies 1-7

Supplementary Derivations

Supplementary Derivation 1: Theoretical derivation of the model for coalescence of dense liquid droplets

Coalescence of dense liquid droplets is a process of energy favourable process because the total free energy will decrease after coalescence. However, if there are impurity particles distributed on the surface of the droplets, the particles will be obstacles for direct contact of the liquid phases, hence prohibiting the coalescence. To realize successful coalescence, an external force *F* is needed to push the droplets together, and “press” the particles into the liquid phases, so that the liquid phases can have direct contact with each other (Fig. 1 in the main text shows the model for the coalescence). In this section we will derive the force *F* necessary to push the impurity particles into the dense liquid phase so that the liquid phases can directly contact with each other.

Fig. 1b shows the force analysis on a particle at the interface between the dense liquid and the bulk solution. *F* is the external force acting on the impurity particle. γ_{bd} is the interfacial tension between the bulk solution and the dense liquid. θ is the contact angle. *R* is the diameter of the impurity particle, and *r* is the distance from the contact point to the vertical line AO. *f* is the vertical component of the interfacial tension γ_{bd}.

If the density of the particles in a unit area at the interface is *n*, then the force F_p (the force on the unit area) necessary to counterbalance the overall interfacial tension will be:

$$\begin{aligned} F_p &= \gamma_{bd}\cos\alpha \cdot 2\pi r \cdot n \\ &= \gamma_{bd}\cos\alpha \cdot 2\pi R \cdot n\cos\beta \\ &= 2\pi n R\gamma_{bd}\cos\alpha \cdot \cos(\pi-\theta-\alpha) \\ &= 2\pi n R\gamma_{bd}(\sin\alpha\cos\alpha\sin\theta - \cos\theta\cos^2\alpha) \end{aligned} \quad (1)$$

It can be derived that, the minimum force of F_p is $\pi R\gamma_{bd}n(1\text{-}\cos\theta)$, which means that, when the force F_p is larger than $\pi R\gamma_{bd}n(1\text{-}\cos\theta)$, the particle will be pushed into the dense liquid phase.

In the model for coalescence of two dense liquid droplets, suppose that under an external force F, the two dense liquids are in direct contact with each other, as shown in Fig. 1c, and at the moment when the diameter of the contact area is R_0 (Fig. 1c), the impurity particles are pushed into the dense liquids, then the force F can be written as follows:

$$F \geq n\pi^2 R R_0^2 \gamma_{bd}(1-\cos\theta) \tag{2}$$

Supplementary Derivation 2: Theoretical derivation of the conditions required for motionless crystallization

At a specific location in the magnet field, a crystal is affected by three forces (Fig. 2b): the buoyancy force (F_b), the magnetic force (F_m) and the gravitational force (G). Since the magnetic field distribution in the horizontal plane is symmetrical, the magnetic force in that plane is cancelled. Therefore, we only need to consider the forces in the vertical direction. The combined force (F) on the crystal in the vertical direction can be written as follow, note that the force is arbitrarily defined positive when it is pointing upward:

$$F = F_b + F_m + G, \tag{3}$$

where

$$F_m = V\frac{\chi_{cryst} - \chi_{sol}}{\mu_0} B\frac{dB}{dy}, \tag{4}$$

$$F_b = \rho_{sol} \cdot V \cdot g, \tag{5}$$

$$G = -\rho_{cryst} \cdot V \cdot g, \tag{6}$$

V is the volume of the crystal; χ_{sol} and χ_{cryst} are the magnetic susceptibility of the solution and the crystal, respectively; ρ_{sol} and ρ_{cryst} are the density of the solution and the crystal, respectively; B is the magnetic field, and dB/dy is the field gradient in the vertical direction (y), μ_0 is the magnetic permeability, which is a constant.

If the combined force (F) is equal to zero, the crystal will be in an equilibrium state, keeping the crystal still. If F is not equal to zero, the crystal will move upward (when $F > 0$), or move downward (when $F < 0$) until $F = 0$.

Suppose $F = 0$ (i.e., the case when the crystal remains motionless), then: $F_b + F_m + G = 0$. Therefore, according to Eqs. (4) - (6), to keep the crystal motionless, the following equation shall be true:

$$\frac{\left(\chi_{cryst} - \chi_{sol}\right)}{\mu_0} B \frac{dB}{dy} + \rho_{sol} \cdot g = \rho_{cryst} \cdot g \tag{7}$$

In Eq. (7), μ_0 is a constant. Since the crystal usually possesses a rigid structure, we can assume that ρ_{cryst} and χ_{cryst} are constant. If the crystal remains still, $B(dB/dy)$ will remain the same. Therefore, in Eq. (7), the actual variables are ρ_{sol} and χ_{sol}.

Eq. (7) can be then simplified as:

$$\frac{\left(\chi_{cryst} - \chi_{sol}\right)}{\left(\rho_{cryst} - \rho_{sol}\right)} = \frac{g \cdot \mu_0}{B \frac{dB}{dy}} = C, \tag{8}$$

where C is a constant.

Eq. (8) is the requirement for keeping the crystal motionless in the solution.

Supplementary Tables

Supplementary Table 1| X-ray diffraction data statistics of lysozyme crystals obtained under non-contact crystallization condition in the superconducting magnet (M1-M5)

	Diffraction data statistics of lysozyme crystals				
	M 1	M 2	M 3	M 4	M 5
Resolution range (Å)	50-1.45 (1.48-1.45)	50-1.49 (1.52-1.49)	50-1.50 (1.53-1.50)	50-1.53 (1.56-1.53)	50-1.56 (1.59-1.56)
Mosaicity (º)	0.39	0.38	0.5	0.45	0.36
$\langle I \rangle / \langle \sigma(I) \rangle$	43.31 (2.04)	50.40 (4.42)	38.81 (2.79)	40.91 (2.15)	34.43 (2.04)
Wilson B (Å^2)	19.9	16.1	13.9	12.8	11.8
Completeness (%)	97.6 (89.9)	97.8 (95.7)	96.6 (96.2)	98.2 (98.1)	98.7 (98.7)
Reflections	145589 (20823)	118176 (19249)	104125 (18683)	135897 (17860)	113034 (17008)
Redundancy	7.0 (4.2)	6.1 (4.8)	5.6 (4.0)	7.6 (5.8)	6.6 (5.1)
R_{merge}	0.372 (0.718)	0.199 (0.506)	0.241 (0.673)	0.396 (0.831)	0.505 (0.943)
Space group	$P4_32_12$	$P4_32_12$	$P4_32_12$	$P4_32_12$	$P4_32_12$
Cell dimension	a = 78.94	a = 78.84	a = 78.93	a = 78.79	a = 78.86
a, b, c (Å)	b = 78.94	bc = 78.84	b = 78.93	b = 78.79	b = 78.86
	c = 37.06	c = 37.05	c = 37.10	c = 37.05	c = 37.11
α, β, γ (°)	$\alpha = \beta = \gamma = 90$	$\alpha = \beta = \gamma = 90$	$\alpha = \beta = \gamma = 90$	$\alpha = \beta = \gamma = 90$	$\alpha = \beta = \gamma = 90$
Exposure time (min)	5	5	5	5	5
Oscillation angle (°)	1	1	1	1	1
Rotation range (°)	90	90	90	90	90
Detector distance (mm)	81	90	81	90	85
Wavelength (Å)	1.54178	1.54178	1.54178	1.54178	1.54178

Values in parentheses are for the highest resolution shell.

Supplementary Table 2| X-ray diffraction data statistics of lysozyme crystals obtained under non-contact crystallization (M6) in the superconducting magnet and the control (C1-C4) outside the magnet

	Diffraction data statistics of lysozyme crystals				
	M 6	C 1	C 2	C 3	C 4
Resolution range (Å)	50-1.57 (1.60-1.57)	50-1.69 (1.72-1.69)	50-1.70 (1.73-1.70)	50-1.73 (1.76-1.73)	50-1.82 (1.84-1.81)
Mosaicity (º)	0.35	0.43	0.42	0.46	0.47
$\langle I\rangle/\langle\sigma(I)\rangle$	38.70 (2.09)	40.17 (2.41)	42.39 (4.69)	32.73 (2.34)	26.59 (2.10)
Wilson B (Å^2)	15.3	17.3	17.1	17.7	19.7
Completeness (%)	99.2 (96.4)	98.3 (83.3)	98.2 (97.5)	97.4 (84.7)	98.8 (90.3)
Reflections	113356 (16809)	107066 (13302)	100305 (13140)	60480 (12493)	71420 (10910)
Redundancy	6.7 (4.9)	8.0 (4.4)	7.6 (6.0)	4.8 (3.1)	6.5 (3.3)
R_{merge}	0.259 (0.693)	0.452 (0.774)	0.429 (0.563)	0.417 (0.604)	0.553 (0.893)
Space group	$P4_32_12$	$P4_32_12$	$P4_32_12$	$P4_32_12$	$P4_32_12$
Cell dimension *a*, *b*, *c* (Å)	a = 78.92 b = 78.92 c = 37.05	a = 78.80 b = 78.80 c = 37.08	a = 78.86 b = 78.86 c = 37.07	a = 79.19 b = 79.19 c = 37.05	a = 78.93 b = 78.93 c = 37.09
α, β, γ (°)	$\alpha = \beta = \gamma = 90$	$\alpha = \beta = \gamma = 90$	$\alpha = \beta = \gamma = 90$	$\alpha = \beta = \gamma = 90$	$\alpha = \beta = \gamma = 90$
Exposure time (min)	5	5	5	5	5
Oscillation angle (°)	1	1	1	1	1
Rotation range (°)	90	90	90	90	90
Detector distance (mm)	90	125	125	130	135
Wavelength (Å)	1.54178	1.54178	1.54178	1.54178	1.54178

Values in parentheses are for the highest resolution shell.

Supplementary Table 3| X-ray diffraction data statistics of lysozyme crystals obtained in the control (C5-C6) outside the magnet

	Diffraction data statistics of lysozyme crystals	
	C 5	C 6
Resolution range (Å)	50-1.86 (1.89-1.86)	50-2.03 (2.07-2.03)
Mosaicity (º)	0.58	0.54
$\langle I\rangle/\langle\sigma(I)\rangle$	32.74 (2.39)	17.83 (2.14)
Wilson B (Å^2)	18.3	15.2
Completeness (%)	96.5 (89.5)	96.3 (98.5)
Reflections	84920 (9986)	74767 (7945)
Redundancy	8.5 (4.7)	9.4 (5.9)
R_{merge}	0.418 (0.893)	0.474 (0)
Space group	$P4_32_12$	$P4_32_12$
Cell dimension *a*, *b*, *c* (Å)	*a* = 79.05 *b* = 79.05 *c* = 37.13	*a* = 78.68 *b* = 78.68 *c* = 37.05
α, *β*, *γ* (°)	*α* = *β* = *γ* = 90	*α* = *β* = *γ* = 90
Exposure time (min)	5	5
Oscillation angle (°)	1	1
Rotation range (°)	90	90
Detector distance (mm)	150	130
Wavelength (Å)	1.54178	1.54178

Values in parentheses are for the highest resolution shell.

Supplementary Table 4| X-ray diffraction data statistics of proteinase K crystals obtained under non-contact crystallization conditions (M1-M3) in the superconducting magnet and the control (C1-C2) outside the magnet

	Diffraction data statistics of proteinase K crystals				
	M 1	M 2	M 3	C 1	C 2
Resolution range (Å)	50-1.51 (1.54-1.51)	50-1.58 (1.61-1.58)	50-1.61 (1.64-1.61)	50-1.75 (1.78-1.75)	50-1.80 (1.83-1.80)
Mosaicity (º)	0.65	0.69	0.68	0.73	0.75
<I>/<σ(I)>	32.43 (2.22)	31.14 (2.01)	33.15 (2.07)	25.25 (2.16)	21.38 (2.21)
Wilson B ($Å^2$)	7.9	11.2	10.19	16.8	16.2
Completeness (%)	96.7 (99.0)	96.7 (99.6)	98.4 (99.9)	99.6 (99.8)	95.9 (97.7)
Reflections	239725 (36541)	227957 (31881)	234509 (30779)	168391 (24635)	179419 (21640)
Redundancy	6.6 (5.5)	7.2 (6.7)	7.6 (7.5)	6.8 (6.6)	8.3 (8.9)
R_{merge}	0.339 (0)	0.456 (0)	0.405 (0)	0.380 (0)	0.323 (0.991)
Space group	$P4_32_12$	$P4_32_12$	$P4_32_12$	$P4_32_12$	$P4_32_12$
Cell dimension *a, b, c* (Å)	*a* = 67.85 *b* = 67.85 *c* = 101.20	*a* = 67.72 *b* = 67.72 *c* = 100.96	*a* = 67.84 *b* = 67.84 *c* = 101.03	*a* = 67.95 *b* = 67.95 *c* = 101.34	*a* = 67.84 *b* = 67.84 *c* = 101.09
α, β, γ (°)	*α* = *β* = *γ* = 90	*α* = *β* = *γ* = 90	*α* = *β* = *γ* = 90	*α* = *β* = *γ* = 90	*α* = *β* = *γ* = 90
Exposure time (min)	5	5	5	5	5
Oscillation angle (°)	1	1	1	1	1
Rotation range (°)	90	90	90	90	90
Detector distance (mm)	85	100	100	100	110
Wavelength (Å)	1.54178	1.54178	1.54178	1.54178	1.54178

Values in parentheses are for the highest resolution shell.

Supplementary Table 5| X-ray diffraction data statistics of proteinase K crystals obtained in the control (C3) outside the magnet

	Diffraction data statistics of lysozyme crystals
	C 3
Resolution range (Å)	50-1.96 (1.99-1.96)
Mosaicity (º)	0.65
<I>/<σ(I)>	21.14 (2.39)
Wilson B (Å^2)	14.65
Completeness (%)	99.8 (99.7)
Reflections	190941 (17587)
Redundancy	10.9 (9.1)
R_{merge}	0.401 (0)
Space group	$P4_32_12$
Cell dimension *a, b, c* (Å)	*a* = 67.81 *b* = 67.81 *c* = 101.12
α, β, γ (°)	*α* = *β* = *γ* = 90
Exposure time (min)	5
Oscillation angle (°)	1
Rotation range (°)	90
Detector distance (mm)	150
Wavelength (Å)	1.54178

Values in parentheses are for the highest resolution shell.

Supplementary Movies

Supplementary Movie 1| Non-contact manipulation of dense liquid droplets using gradient magnetic field generated by a cylindrical permanent magnet. The magnet is placed at the left side of the sample with phase-seperated dense liquid droplets. It can be seen that the dense liquid droplets were pushed by the magnet to the right side where the magnetic field is low.

Supplementary Movie 2| Non-contact manipulation of dense liquid droplets using gradient magnetic field generated by an N-N permanent magnet pair. The sample with phase-seperated dense liquid droplets is placed between the two magnets. It can be seen that the dense liquid droplets were pushed to the center where the magnetic field is low.

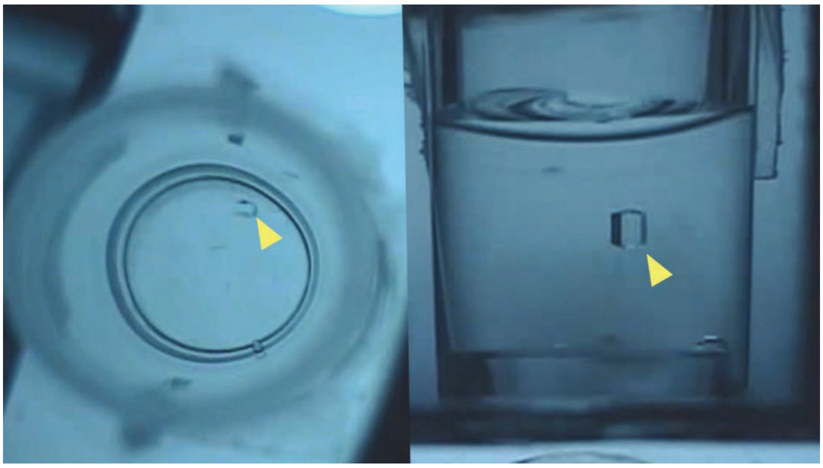

Supplementary Movie 3| The nucleation and growth of a lysozyme single crystal in superconducting magnet monitored by *in-situ* CCD cameras. (a) Top view. (b) Side view. The movie is a shortened version from a 4 days' experiment. The yellow arrow indicates the single crystal.

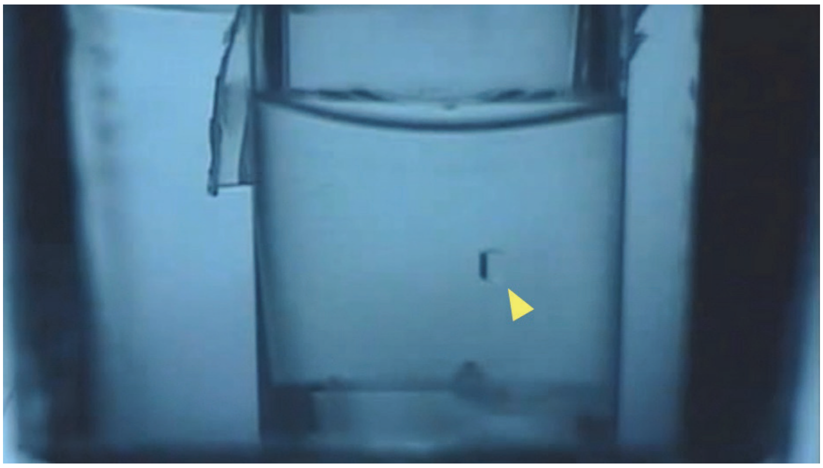

Supplementary Movie 4| The nucleation and growth of a lysozyme single crystal in superconducting magnet monitored by *in-situ* CCD cameras. The movie is a shortened version from a 2 days' experiment. The yellow arrow indicates the single crystal.

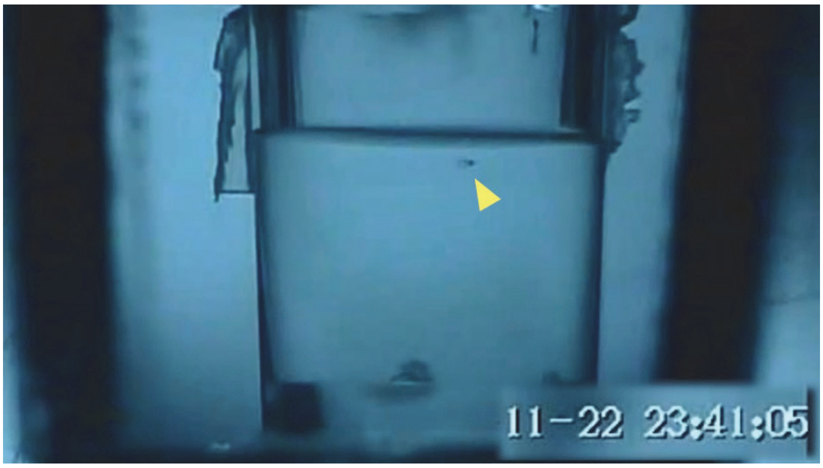

Supplementary Movie 5| The nucleation and growth of a proteinase K single crystal in superconducting magnet monitored by *in-situ* CCD cameras. The movie is a shortened version from a 1 day’s experiment. The yellow arrow indicates the single crystal.

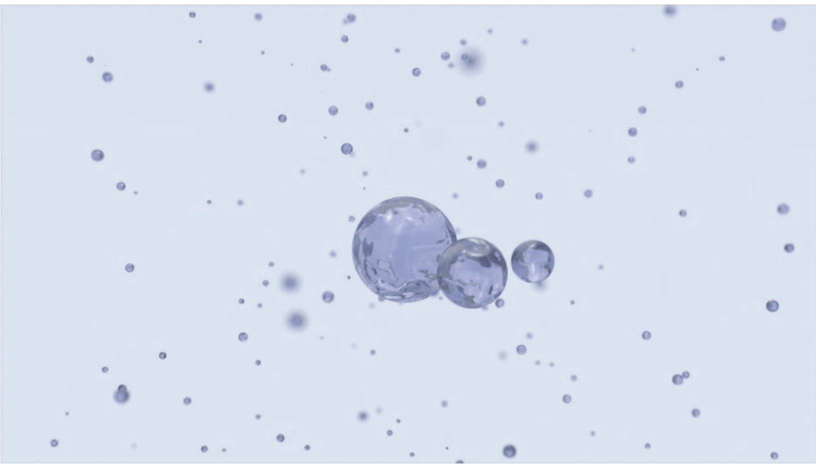

Supplementary Movie 6| An animation movie demonstrating the non-contact crystallization process from solution under directed magnetic force. The movie starts from liquid-liquid phase separation (LLPS) process, in which small droplets of dense liquids form. The droplets will grow via collisions & coalescence or via incorporation of solutes from surrounding bulk solution. Simultaneously, larger dense liquid droplets will be pushed by the magnetic force to the localized low magnetic field, where the droplets will merge together, leading to the formation of a large single dense liquid drop, from which a single suspended crystal will nucleate and grow in a fully non-contact manner.

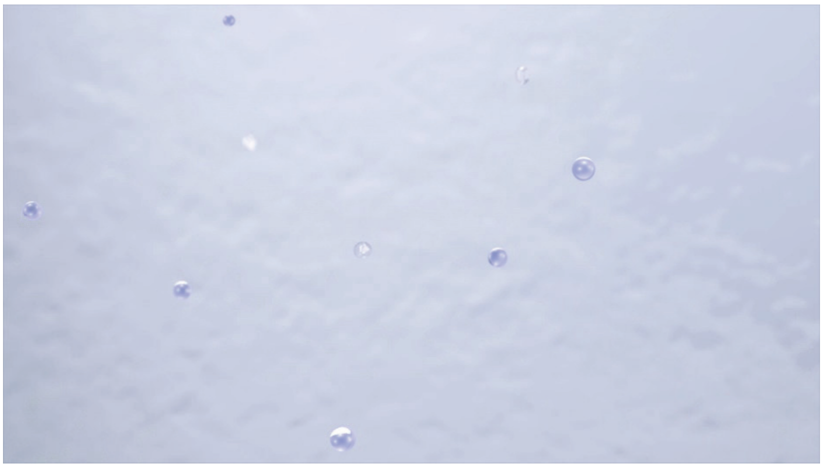

Supplementary Movie 7| An animation movie demonstrating the crystallization process from solution under the normal conditions. The movie starts from liquid-liquid phase separation (LLPS) process, in which small droplets of dense liquids form. The droplets will grow via collisons & coalescence or via incorporating solutes from surrounding bulk solution. Nucleation of crystals will occur in the dense liquid droplets when the size of the droplets is large enough. Grown crystals (and also the dense liquid droplets) will sediment to the bottom of the container when their size is large enough.